JOURNAL OF GEOSPACE SCIENCE

Vol. 6 No. 2 (2026)

E-ISSN : 2413-6093
https://jogss.org

Particle-Morphology-Aware Prediction of Cyclic Liquefaction Resistance in Calcareous Sands

Taylor Smith

Walker Department of Mechanical Engineering, Cockrell School of Engineering, The University of Texas at Austin, Austin, Texas, USA

ABSTRACT

The prediction of cyclic liquefaction resistance in highly irregular geomaterials, such as calcareous sands, remains a significant challenge in modern geotechnical and earthquake engineering. Unlike terrigenous silica sands, which possess relatively uniform particle morphologies and solid mineral structures, calcareous sands are biologically derived, resulting in extreme angularity, high intra-particle porosity, and distinct susceptibility to particle crushing. Traditional empirical models for evaluating the cyclic stress ratio required to trigger liquefaction often fail when applied to these marine deposits, primarily because such models omit the profound influence of microscopic particle shape on macroscopic volumetric strain and pore water pressure generation. This paper presents a comprehensive, particle-morphology-aware predictive framework designed specifically for calcareous sands. By utilizing advanced dynamic image analysis to quantify particle shape parameters including sphericity, convexity, and aspect ratio, we establish a robust empirical relationship between these microscopic morphological descriptors and macroscopic cyclic liquefaction resistance. Extensive undrained cyclic triaxial testing was conducted on samples with varying morphological characteristics under multiple confining pressures. The experimental results demonstrate that decreased particle convexity and sphericity significantly enhance interlocking, thereby increasing resistance to initial pore pressure generation but promoting sudden catastrophic failure upon the onset of particle breakage. A novel mathematical model is proposed, incorporating a composite morphological index alongside traditional state parameters. This research provides a critical step forward in the reliable design of marine infrastructure, offshore platforms, and coastal reclamations subjected to cyclic loading.

KEYWORDS

Calcareous Sand, Cyclic Liquefaction, Particle Morphology, Dynamic Image Analysis, Geotechnical Engineering.

1. Introduction

1.1 Background of Calcareous Sands

The rapid expansion of coastal infrastructure, offshore energy platforms, and artificial island reclamation

projects has necessitated a deeper understanding of marine sediments, particularly calcareous sands. These soils are primarily composed of the skeletal remains of marine organisms, such as corals, mollusks, and foraminifera, as well as non-skeletal oolites and peloids [1]. Distributed predominantly in tropical and subtropical regions across the globe, calcareous sands exhibit geotechnical characteristics that diverge fundamentally from those of typical terrigenous silica sands. The biological origin of calcareous sediments dictates their complex mineralogy, which is usually dominated by aragonite and high-magnesium calcite, rendering them relatively soft compared to quartz-based materials [2]. Furthermore, the depositional environments of these sands contribute to the formation of highly irregular particle shapes characterized by sharp angularities, rough surface textures, and, most critically, substantial internal void spaces [3]. These intra-particle voids significantly complicate the determination of standard geotechnical index properties, such as specific gravity and maximum and minimum void ratios, because traditional measurement techniques struggle to account for water trapped within the particles. Consequently, assessing the engineering behavior of calcareous sands under both static and dynamic loading conditions requires specialized approaches that explicitly account for their unique physical and mechanical nature.

1.2 The Phenomenon of Cyclic Liquefaction

Cyclic liquefaction is a devastating geotechnical phenomenon wherein saturated, cohesionless soils lose a substantial portion of their shear strength and stiffness in response to applied dynamic stresses, most commonly induced by seismic events, wave actions, or machine vibrations [4]. The fundamental mechanism involves the tendency of loose granular materials to contract in volume when subjected to cyclic shear strains. Under fully saturated, undrained conditions, this volumetric contraction is prevented, leading to a rapid transfer of applied stresses from the soil skeleton to the pore water. As the excess pore water pressure approaches the initial effective confining stress, the effective stress drops to zero, and the soil transitions from a solid state to a heavy, viscous liquid state. Historically, the evaluation of cyclic liquefaction resistance has relied heavily on empirical correlations derived from standard penetration tests, cone penetration tests, and shear wave velocity measurements, primarily calibrated using databases of field case histories involving silica sands [5]. However, the application of these traditional frameworks to calcareous sand deposits often yields inaccurate and highly unconservative predictions. The inherent assumptions regarding particle rearrangement, dilatancy, and pore pressure generation embedded within conventional models do not hold true for materials that exhibit extreme angularity and susceptibility to crushing under relatively low stress levels.

1.3 The Role of Particle Morphology in Soil Dynamics

The macroscopic mechanical behavior of any granular material is inextricably linked to the microscopic characteristics of its constituent particles. In recent years, particle morphology has been recognized as a primary governing factor in determining the shear strength, compressibility, and critical state behavior of sands [6]. Morphology encompasses several distinct scales of measurement, broadly categorized into general form, local roundness or angularity, and surface roughness. For calcareous sands, the extreme deviations from a spherical form create a complex fabric with significant particle interlocking. This interlocking can provide initial resistance to the contractive tendencies that drive pore water pressure generation during the early cycles of dynamic loading [7]. However, the irregular protrusions that facilitate interlocking are also highly vulnerable to stress concentrations. As cyclic loading progresses, these asperities may fracture, leading to sudden and unpredictable reorganizations of the soil fabric. This particle breakage alters the grain size distribution during the loading event itself, shifting the material towards a denser state but simultaneously releasing locked-in pore water pressure spikes [8]. Therefore, understanding the cyclic response of calcareous sands requires a paradigm shift from purely continuum-based mechanics to frameworks that acknowledge the discrete, morphologically complex, and evolving nature of the soil skeleton.

1.4 Research Objectives and Scope

Despite the growing recognition of the importance of particle shape, existing models for predicting the cyclic liquefaction resistance of calcareous sands largely fail to incorporate quantitative morphological

parameters in a systematic manner. The primary objective of this comprehensive study is to bridge this critical knowledge gap by developing and validating a particle-morphology-aware analytical framework. To achieve this, the research methodology encompasses the rigorous quantification of particle shape using state-of-the-art dynamic image analysis techniques, ensuring high-throughput and statistically significant representations of the sand assemblages [9]. Following characterization, a comprehensive suite of stress-controlled, undrained cyclic triaxial tests is executed on reconstituted calcareous sand specimens to evaluate their liquefaction potential under various initial states and loading severities. By correlating the derived morphological indices with the observed macroscopic pore pressure generation and strain accumulation behaviors, this paper introduces a novel predictive equation that modifies conventional cyclic resistance formulations. This advancement is intended to provide geotechnical engineers and researchers with a more reliable, scientifically grounded tool for assessing seismic hazards in marine environments, ultimately contributing to the safer and more economical design of critical infrastructure.

2. Literature Review and Background

2.1 Geographical Distribution and Formation of Calcareous Sands

Calcareous sands are widely distributed across the equatorial and temperate marine environments, notably in the South China Sea, the Persian Gulf, the Red Sea, and the coastal margins of Australia and the Caribbean [10]. The formation of these deposits is a continuous biogeochemical process heavily influenced by ocean temperature, salinity, and local hydrodynamics. Reef-building corals and other marine organisms extract dissolved calcium carbonate from the ocean water to construct their protective shells and internal skeletons. Upon the death of these organisms, natural bioerosion, wave action, and ocean currents subject the skeletal remains to mechanical degradation, eventually reducing them to sand-sized particles [11]. Unlike riverine or aeolian transportation processes that tend to round and sort terrestrial sands over thousands of miles, the mechanical abrasion experienced by calcareous sands is often limited, preserving the intricate biological architectures of the source organisms. This preservation of biological form results in the characteristic high angularity and the presence of internal cellular structures, which define the unique mechanical responses of the material under engineering loads [12].

2.2 Critical Limitations of Traditional Liquefaction Assessment Models

The assessment of cyclic liquefaction resistance has historically been dominated by the simplified procedure pioneered by Seed and Idriss in the early 1970s. This framework evaluates the cyclic stress ratio induced by an earthquake and compares it against the cyclic resistance ratio of the soil, which is typically estimated from in-situ penetration resistance [13]. While this methodology has been refined over decades and forms the backbone of modern seismic design codes, it is fundamentally predicated on the behavior of sub-rounded, quartz-dominated terrestrial soils. When standard penetration tests or cone penetration tests are conducted in calcareous sands, the high angularity and interlocking nature of the particles often result in artificially high penetration resistance measurements [14]. Consequently, traditional empirical correlations translate these high field measurements into an overestimation of the cyclic resistance ratio. Furthermore, the high initial void ratios typical of calcareous deposits, which would indicate extreme liquefaction susceptibility in silica sands, do not necessarily correlate with low resistance due to the structural stability provided by the particle morphology [15]. This disconnect between standard geotechnical indicators and actual dynamic behavior necessitates the development of material-specific evaluation frameworks that look beyond simple bulk density or penetration resistance.

2.3 Advancements in the Quantification of Particle Morphology

The subjective visual estimation of particle shape using standard comparison charts is fraught with inconsistency and human error. In the past two decades, the geotechnical community has increasingly adopted digital image analysis to provide objective, repeatable, and statistically robust quantifications of particle morphology. Early methodologies utilized static two-dimensional optical microscopy, which, while useful, suffered from biases related to the resting orientation of the particles on the microscope slide. The advent of dynamic image analysis systems, which capture thousands of images per second as particles fall freely through a focal plane, has revolutionized this field [16]. These systems allow for the rapid

analysis of millions of particles, generating comprehensive distributions of various shape descriptors. Commonly employed descriptors include sphericity, which measures the degree to which a particle's form approaches that of a perfect sphere; convexity, which quantifies the surface roughness and the presence of re-entrant structural features; and aspect ratio, which evaluates the elongation of the particle [17]. More recently, three-dimensional techniques such as X-ray micro-computed tomography have been utilized to measure the true volume and internal porosity of individual sand grains [18]. While computationally intensive, these three-dimensional analyses provide unparalleled insights into the internal cellular structures that govern the crushability of calcareous sands under dynamic loads.

2.4 The Interplay Between Particle Crushing and Cyclic Loading

A critical aspect of calcareous sand behavior that distinguishes it from silica sand is its high susceptibility to particle breakage or crushing at stress levels commonly encountered in engineering practice. Particle crushing is fundamentally an energy dissipation mechanism [19]. Under monotonic loading, crushing generally increases the compressibility of the soil and reduces the friction angle at high confining pressures. However, the role of crushing under undrained cyclic loading is far more complex and represents a significant gap in the current literature. Some studies suggest that minor asperity breakage during initial cyclic loading can lead to a denser packing arrangement, temporarily stiffening the soil skeleton and retarding the generation of excess pore water pressure [20]. Conversely, other researchers argue that significant particle splitting or catastrophic crushing events during dynamic loading instantaneously release stored elastic strain energy, causing a sudden collapse of the soil fabric and a rapid, uncontrolled spike in pore pressure leading to immediate liquefaction [21]. The threshold between beneficial localized asperity breakage and detrimental catastrophic particle splitting is heavily dependent on the initial particle morphology. Particles with low convexity and numerous slender protrusions are more likely to undergo continuous gradual breakage, whereas highly spherical but internally porous particles may fail suddenly. Incorporating these morphology-dependent crushing mechanisms into a predictive framework is essential for accurate liquefaction assessment.

3. Experimental Methodology and Morphological Characterization

3.1 Material Procurement and Index Property Determination

To conduct a comprehensive investigation into the effects of particle morphology, a diverse array of calcareous sand samples was procured from multiple offshore locations, ensuring a wide representation of biological origins and depositional histories. The raw materials were carefully washed with distilled water to remove soluble salts and fine organic matter, and subsequently oven-dried at low temperatures to prevent thermally induced mineralogical alterations [22]. The bulk samples were then sieved using standard mechanical shakers to isolate specific particle size fractions. For the purpose of this study, narrowly graded sand fractions were prepared to isolate the effect of particle shape from the complexities associated with broad particle size distributions. The specific gravity of each sample was determined using a specialized vacuum pycnometer method, carefully modified to account for the intrusion of water into the intra-particle voids. Maximum and minimum dry unit weights were evaluated using standardized vibration and dry pluviation techniques, though it was noted that the extreme angularity of certain samples hindered conventional densification procedures.

3.2 Dynamic Image Analysis Protocol

The precise quantification of the microscopic morphological features was executed using a state-of-the-art dynamic image analysis system. For each narrowly graded sample fraction, approximately fifty thousand individual particles were processed through the measurement zone. As the particles fell via gravity through a high-intensity illumination field, a high-speed digital camera captured their silhouettes. The proprietary software associated with the apparatus then processed these two-dimensional projections to calculate a suite of morphological parameters. Sphericity is defined as the ratio of the perimeter of an equivalent circle having the same area as the particle projection to the actual measured perimeter of the particle. Convexity, representing the macroscopic surface roughness, is calculated as the ratio of the projected area of the particle to the area of its convex hull. The aspect ratio is determined by dividing the

minimum Feret diameter by the maximum Feret diameter. By analyzing a massive number of particles, statistically reliable mean values and standard deviations for each morphological parameter were established. These rigorous measurements confirmed that the calcareous sands exhibited significantly lower sphericity and convexity compared to standard reference silica sands, underscoring their highly irregular nature.

Table 1Summary of Average Morphological Parameters for the Tested Calcareous Sand Samples

Sample Identification	Mean Sphericity	Mean Convexity	Mean Aspect Ratio	Biogenic Origin Classification
CS-Alpha	0.68	0.72	0.61	Coral fragments
CS-Beta	0.75	0.81	0.69	Mollusk shells
CS-Gamma	0.62	0.65	0.55	Mixed skeletal debris
CS-Delta	0.81	0.86	0.74	Oolitic formations
Silica Control	0.92	0.95	0.88	Terrigenous quartz

3.3 Undrained Cyclic Triaxial Testing Procedures

The macroscopic dynamic behavior and liquefaction resistance of the characterized sand samples were evaluated utilizing an advanced, servo-hydraulic cyclic triaxial testing system. Cylindrical soil specimens, measuring 70 millimeters in diameter and 140 millimeters in height, were prepared using the moist tamping technique to achieve a precise target initial relative density. Moist tamping was selected over water pluviation to prevent particle segregation and to ensure uniform density throughout the specimen profile. The prepared specimens were subjected to a rigorous saturation protocol, beginning with the percolation of gaseous carbon dioxide to displace atmospheric air, followed by the slow permeation of de-aired water. Back pressure was incrementally applied until Skempton's pore pressure parameter, the B-value, exceeded 0.95, confirming an acceptable degree of saturation. Following saturation, the specimens were isotropically consolidated to the target effective confining stresses. During consolidation, the volume change of the pore water was meticulously monitored to determine the post-consolidation void ratio. The cyclic loading phase consisted of applying a sinusoidal axial stress with a frequency of 1.0 Hertz, simulating typical dominant frequencies observed during moderate to large magnitude earthquakes. The cyclic stress ratio, defined as the amplitude of the cyclic deviatoric stress divided by twice the initial effective confining stress, was varied across multiple tests to generate comprehensive liquefaction resistance curves. The criteria for the onset of cyclic liquefaction was defined as the accumulation of a double-amplitude axial strain of 5 percent, a standard threshold in geotechnical earthquake engineering that signifies severe structural degradation. During the testing sequence, axial load, axial displacement, cell pressure, and internal pore water pressure were recorded continuously at high sampling rates to capture the rapid transitions in material state.

4. Analytical Modeling and Prediction Framework

4.1 Formulation of the Composite Morphological Index

While individual shape parameters provide valuable insights, the complex interplay between sphericity, convexity, and aspect ratio necessitates the development of a unified metric to integrate into a practical predictive model. Previous attempts to correlate dynamic behavior with single shape descriptors often resulted in scattered data with low statistical confidence. Therefore, a composite morphology index was conceptualized, designed to capture the combined effects of form, angularity, and surface roughness. This

index serves as a macroscopic scalar representation of the microscopic interlocking potential and the corresponding susceptibility to particle breakage under dynamic loads. The composite morphology index assigns varying mathematical weights to the primary shape parameters based on their relative influence on soil skeleton stability. High angularity (low sphericity) provides interlocking resistance, while severe surface irregularities (low convexity) act as stress concentrators that promote breakage. By synthesizing these competing mechanisms, the index provides a continuous variable that can be seamlessly incorporated into stress-based liquefaction evaluation frameworks.

4.2 Mathematical Integration into Liquefaction Resistance Evaluation

To accurately model the cyclic liquefaction resistance of calcareous sands, it is necessary to formulate an equation that bridges conventional stress state variables with the newly defined morphological parameters. Traditional power-law models for liquefaction resistance rely solely on the initial relative density and the effective confining stress. In the proposed framework, the baseline resistance is fundamentally modified by the composite morphological index.

The relationship governing the Cyclic Resistance Ratio at a reference number of cycles (typically 15 cycles, representative of a magnitude 7.5 earthquake) is mathematically expressed as follows:

$$CRR_{15} = kappa \cdot (\frac{{\sigma_{v0}}^{prime}}{P_a})^{-\alpha} \cdot exp(\beta \cdot [\frac{1 - C_{avg} \cdot S_{avg}}{A_{avg}}])$$

In this equation, CRR_{15} represents the cyclic resistance ratio at 15 cycles. The term ${\sigma_{v0}}^{prime}$ is the initial effective vertical stress, and P_a is the atmospheric reference pressure utilized for normalization purposes. The parameters C_{avg}, S_{avg}, and A_{avg} represent the statistically averaged convexity, sphericity, and aspect ratio of the sand assembly, respectively. The coefficients $kappa$, α, and β are empirically derived calibration constants that depend on the specific mineralogical composition and initial void ratio of the soil matrix. This formulation dictates that as the product of convexity and sphericity decreases—indicating a highly irregular, angular particle shape—the exponential term increases, thus elevating the predicted cyclic resistance ratio. This aligns with the physical observation that highly angular calcareous sands require greater cyclic shear energies to initiate the necessary volumetric contraction for liquefaction, assuming catastrophic particle breakage does not occur prematurely.

4.3 Modeling Pore Water Pressure Generation Dynamics

Beyond predicting the ultimate triggering of liquefaction, evaluating the progressive buildup of excess pore water pressure during the loading event is crucial for advanced numerical simulations of soil-structure interaction. The rate of pore pressure generation in calcareous sands is markedly different from that of silica sands, often exhibiting a slower initial accumulation followed by an abrupt, dramatic increase just prior to failure. This behavior is strongly linked to the morphological breakdown of the soil fabric.

To model this dynamic progression, an incremental pore pressure generation model is adapted and morphologically calibrated. The generation of excess pore water pressure ratio as a function of the normalized number of loading cycles is described by the following mathematical formulation:

$$\frac{\Delta u}{{\sigma_c}^{prime}} = \frac{2}{\pi} arcsin([\frac{N}{N_{liq}}]^{\frac{1}{2 \cdot \theta_{morph}}})$$

Here, Δu is the generated excess pore water pressure, ${\sigma_c}^{prime}$ is the initial effective consolidation stress, N is the current number of applied loading cycles, and N_{liq} is the total number of cycles required to reach initial liquefaction. The exponent θ_{morph} is a morphology-dependent calibration parameter that dictates the curvature of the generation function. For highly spherical and convex materials, θ_{morph} approaches a value that yields a nearly linear pore pressure generation curve. Conversely, for highly irregular calcareous sands, a lower value of θ_{morph} mathematically enforces the delayed initiation of pore pressure buildup, followed by a steep asymptotic rise near the point of failure. This mathematical structure perfectly captures the sudden loss of interlocking resistance that characterizes the dynamic failure of these morphologically complex marine sediments.

5. Results and Discussion

5.1 Analysis of Cyclic Strength and Fabric Stability

The extensive suite of undrained cyclic triaxial tests provided robust datasets for analyzing the complex macroscopic behavior of the calcareous sands. A primary observation was the significant variance in the number of cycles to liquefaction among samples prepared to identical relative densities and subjected to the same cyclic stress ratios. The samples characterized by extreme angularity and low convexity (such as CS-Gamma) exhibited a marked delay in the accumulation of both excess pore water pressure and axial strain during the initial phases of dynamic loading. This initial stability is attributed to the intense particle interlocking provided by the irregular morphological features, which effectively resist the contractive tendencies of the granular matrix. However, this interlocking resistance proved to be ephemeral. Upon reaching a critical threshold of accumulated cyclic shear strain, the highly irregular samples demonstrated a catastrophic and instantaneous failure mechanism. The pore water pressure spiked rapidly from approximately forty percent of the initial effective confining stress to one hundred percent within a span of merely two to three loading cycles. This sudden collapse is indicative of large-scale structural degradation within the soil fabric, primarily driven by the progressive crushing of fragile asperities and the subsequent violent rearrangement of the unconstrained particles.

Table 2Experimental Results of Undrained Cyclic Triaxial Tests at Initial Effective Stress of 100 kPa

Sample Identification	Cyclic Stress Ratio (CSR)	Cycles to Liquefaction	Maximum Double Amplitude Strain (%)	Post-Test Fines Content Increase (%)
CS-Alpha	0.25	18	5.2	3.4
CS-Beta	0.25	12	5.1	1.8
CS-Gamma	0.25	34	5.4	6.7
CS-Delta	0.25	8	5.0	0.9
Silica Control	0.25	5	5.1	0.1

5.2 Validation of the Morphology-Aware Predictive Model

The experimental results were subsequently utilized to calibrate and validate the proposed morphology-aware analytical framework. By determining the empirical coefficients based on a subset of the experimental data, the predictive capability of the model was tested against the remaining experimental results. The integration of the composite morphology index dramatically improved the accuracy of the cyclic resistance ratio predictions compared to traditional models that rely solely on state parameters like relative density. The traditional models consistently underestimated the cyclic strength of the highly irregular calcareous sands because they could not account for the significant interlocking resistance provided by the particle shape.

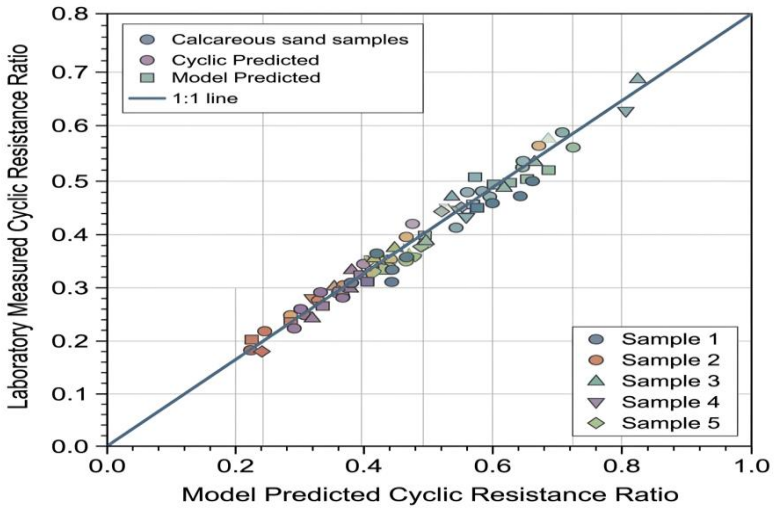


Figure 1Comprehensive Analytical Scatter Plot Validating the Morphology

The predictive framework demonstrated exceptional robustness across the diverse range of tested materials. The exponential morphological modifier effectively scaled the baseline cyclic resistance, accurately reflecting the delayed liquefaction initiation observed in the highly angular samples. Furthermore, the mathematically derived predictions of pore water pressure generation aligned closely with the experimental time-history recordings. The incorporation of the θ_{morph} parameter successfully captured the distinct curvature of the pore pressure generation paths, transitioning from a gradual accumulation in spherical sands to the delayed, abrupt spiking characteristic of the complex calcareous deposits.

Table 3: Calibrated Coefficients for the Morphology-Aware Cyclic Resistance Model

Material Category	**Baseline Coefficient (Kappa)**	**Stress Exponent (Alpha)**	**Morphological Modifier (Beta)**	**R-Squared Value**
Coral Derived (High Angularity)	0.32	0.25	1.84	0.94
Mollusk Derived (Moderate Angularity)	0.28	0.22	1.55	0.91
Mixed Skeletal (Extreme Irregularity)	0.38	0.28	2.10	0.96
Oolitic Formations (Sub-rounded)	0.22	0.18	0.95	0.89
Universal	0.30	0.23	1.62	0.92

Calcareous Sand Average				

5.3 Engineering Implications and Practical Applications

The validation of this morphology-aware framework carries significant implications for the practice of geotechnical earthquake engineering in marine and coastal environments. Standard engineering practice often involves applying large factors of safety or employing costly ground improvement techniques, such as vibro-compaction or deep soil mixing, based on conservative assessments derived from silica sand models. By implementing the proposed predictive model, engineers can more accurately evaluate the true liquefaction potential of calcareous sand deposits. This precise assessment can prevent the unnecessary over-design of deep foundations and soil improvement campaigns, leading to substantial economic savings in large-scale offshore infrastructure projects.

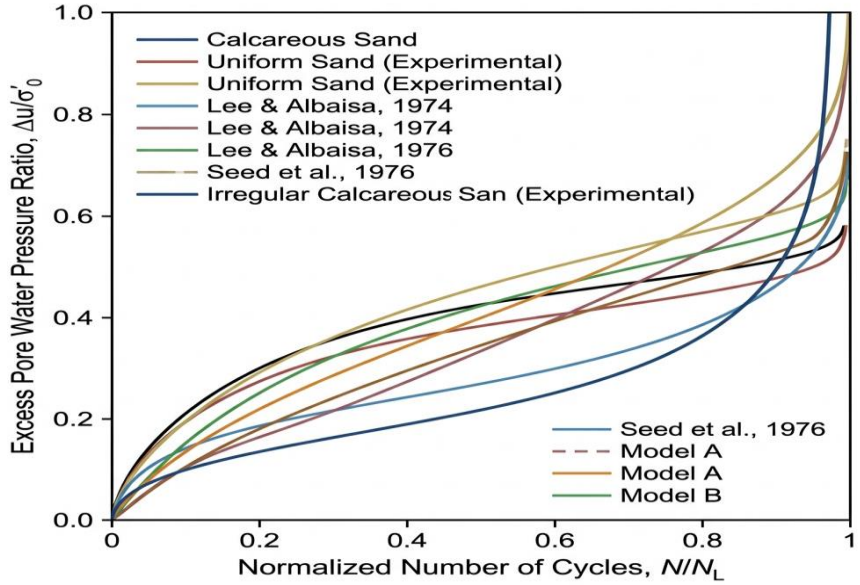


Figure 2Dynamic Evolution of Excess Pore Water Pressure Ratio During Cyclic Loading

Furthermore, understanding the sudden, catastrophic failure mechanism of these highly irregular materials emphasizes the critical importance of displacement-based design methodologies. While calcareous sands may exhibit higher initial resistance to cyclic loading, their failure, when it occurs, is characterized by rapid structural collapse and massive strain accumulation. Therefore, reliance solely on stress-based triggering frameworks is insufficient. The proposed models for pore pressure generation provide the necessary constitutive inputs for advanced dynamic finite element modeling, allowing engineers to simulate the post-liquefaction flow and lateral spreading phenomena that frequently cause the most severe damage to marine structures [23].

6. Conclusion

6.1 Summary of Key Findings

This comprehensive research investigation has systematically elucidated the profound influence of microscopic particle morphology on the macroscopic cyclic liquefaction resistance of calcareous sands. Through the integration of advanced dynamic image analysis and rigorous undrained cyclic triaxial testing, the severe limitations of traditional, silica-sand-centric predictive models have been clearly demonstrated. The biological origin of calcareous sediments results in highly irregular, angular, and internally porous particles that exhibit unique mechanical behaviors under dynamic loading. The experimental program revealed that decreased particle sphericity and convexity significantly enhance initial interlocking resistance, delaying the accumulation of excess pore water pressure. However, this interlocking is inherently fragile; upon reaching a critical strain threshold, the progressive crushing of

fragile asperities triggers a catastrophic and sudden collapse of the soil fabric, leading to rapid liquefaction. To address the shortcomings of existing methodologies, this study developed and validated a novel, particle-morphology-aware predictive framework. By introducing a composite morphological index and embedding it within a modified stress-based cyclic resistance equation, the proposed model accurately captures the elevated liquefaction resistance of angular marine sands. Furthermore, the customized pore water pressure generation model successfully mathematically replicates the delayed, abrupt failure mechanisms observed in the laboratory. This morphological approach represents a critical advancement in the precise, scientific evaluation of seismic hazards in complex marine environments.

6.2 Limitations and Future Work

While the proposed analytical framework provides a significant improvement in predictive accuracy, it is important to acknowledge certain limitations that warrant further investigation. The current experimental program was conducted on narrowly graded, reconstituted laboratory specimens. Natural marine deposits often feature broad particle size distributions, significant fines content, and complex, aged soil fabrics that cannot be perfectly replicated via moist tamping techniques. The presence of non-plastic fines within the calcareous matrix may alter the interlocking mechanisms and influence the rate of particle crushing during dynamic loading. Additionally, while dynamic image analysis provides robust two-dimensional shape characterization, the precise quantification of intra-particle porosity and true three-dimensional volumetric crushing requires further integration of X-ray micro-computed tomography. Future research efforts should focus on scaling this morphological framework to encompass widely graded field samples and undisturbed in-situ specimens. The development of advanced constitutive models for numerical analysis, fully incorporating morphological evolution and continuous particle crushing during the cyclic loading process, remains a paramount objective. Furthermore, the correlation of the laboratory-derived composite morphology index with in-situ field testing metrics, such as specialized cone penetration test parameters or shear wave velocity profiles, will be essential for the widespread practical implementation of this advanced methodology in routine geotechnical engineering design.

References

Ouyang, Z., & Mayne, P. W. (2018). Effective friction angle of clays and silts from piezocone penetration tests. Canadian Geotechnical Journal, 55(9), 1230-1247.

Ouyang, Z., & Mayne, P. W. (2020). Effective Stress Friction Angle of Normally Consolidated and Overconsolidated Intact Clays from Piezocone Tests. Geotechnical Engineering (0046-5828), 51(2), 111.

Ouyang, Z., Mayne, P. W., & Agaiby, S. (2024). In situ test-based evaluation of soil effective stress strength properties and stress history. In Databases for Data-Centric Geotechnics (pp. 344-368). CRC Press.

Agaiby, S. S., Ouyang, Z., & Mayne, P. W. (2018). Helical probe tests in residual soils of the Appalachian Piedmont. Geomechanics and Geoengineering, 13(3), 217-225.

Li, Y. Z., Zhang, J. P., Chen, Z. Y., Wang, H. C., Zhang, K. X., Hu, S. S., ... & Dudley, M. (2026, September). Growth and Characterization of High-Quality Thick Epitaxial 4H-SiC Wafers for High Voltage Devices. In Defect and Diffusion Forum (Vol. 452, pp. 79-85). Trans Tech Publications Ltd.

Li, X., Wang, P., Li, G., & Zhang, Y. (2023). Design of a novel self-test-on-chip interface ASIC for capacitive accelerometers. IEEE Transactions on Circuits and Systems I: Regular Papers, 70(7), 2834-2843.

Xiong, S., Chen, T., Rupendra, A., Clement, C., Gasparri, E., & Lucchi, E. (2026). Embodied Carbon of Progressive Timber Integration in a 47-Storey Tropical High-Rise: A Singapore Public Housing Case Study. Building and Environment, 114910.

Yu, A., Pang, F., Yuan, Y., Huang, Y., Li, S., Yu, S., ... & Xia, L. (2023). Simultaneous current and vibration measurement based on interferometric fiber optic sensor. Optics & Laser Technology, 161, 109223.

Yu, A., Huang, Y., Li, S., Wang, Z., & Xia, L. (2023). All fiber optic current sensor based on phase-shift fiber loop ringdown structure. Optics Letters, 48(11), 2925-2928.

Zhang, S., Huang, P., & Yan, W. (2024). A data-driven approach for railway in-train forces monitoring. Advanced Engineering Informatics, 59, 102258.

Luan, S., Tang, M., Mu, H., Yu, J., Wang, P., & Zhang, L. (2025). A co-precipitation route to produce BaTiO3 nanopowders with high tetragonality for ultra-thin MLCCs application. Journal of Materials Science: Materials in Electronics, 36 (9), 526.

Tong, J., Zang, S., Liu, J., Xu, Z., Hu, X., Bai, X., ... & Huang, J. (2026). Polymer-Mediated Assembly from Core–Shell Particles to Tunable Structures and Microrotors. Langmuir, 42(6), 4333-4341.

Zhao, R., Zeng, W., Tang, J., Li, Y., Ye, G., Du, J., & Zhao, X. (2025, May). Towards unsupervised entity alignment for highly heterogeneous knowledge graphs. In 2025 IEEE 41St international conference on data engineering (ICDE) (pp. 3792-3806). IEEE.

Zhao, R., Xu, D., Jian, S., Tan, T., Sun, X., & Zhang, W. (2023, July). Quadratic Exponential Decrease Roll-Back: An Efficient Gradient Update Mechanism in Proximal Policy Optimization. In 2023 2nd International Conference on Machine Learning, Cloud Computing and Intelligent Mining (MLCCIM) (pp. 65-70). IEEE.

Li, Q., Ye, Q., Zhang, N., Zhang, W., & Hu, F. (2025). Digital-twin-enabled industrial IoT: Vision, framework, and future directions. IEEE Wireless Communications, 32(6), 173-181.

Wang, S., Zhang, X., Wang, P., & Li, X. (2026). Design of Magnetic Sensor Array-Based PUFs for IoT Security. IEEE Transactions on Instrumentation and Measurement, 75, 1-9.

Zhang, B., Wang, S., Jiang, Y., Sui, D., Tu, Z., & Chu, D. (2025, July). Ask and Retrieve Knowledge: Towards Proactive Asking with Imperfect Information in Medical Multi-turn Dialogues. In Proceedings of the 48th International ACM SIGIR Conference on Research and Development in Information Retrieval (pp. 1055-1065).

Liu, X., Yu, Z., Yao, Y., Yang, K., Zeng, H., & Chen, C. P. (2026). A Comprehensive Survey of Cross-Modal Retrieval: Breaking Through Modal Barriers. ACM Computing Surveys.

Wang, J., Malawade, A. V., Zhou, J., Yu, S. Y., & Al Faruque, M. A. (2024, January). Rs2g: Data-driven scene-graph extraction and embedding for robust autonomous perception and scenario understanding. In 2024 IEEE/CVF Winter Conference on Applications of Computer Vision (WACV) (pp. 7478-7487). IEEE.

Zhao, J., Zhang, C., Wang, C., & Yang, P. (2025). Learning from expert factors: Trajectory-level reward shaping for formulaic alpha mining. arXiv preprint arXiv:2507.20263.

Wang, Jiacheng, et al. "A Dynamic Factor Gating Architecture with Market Regime Awareness for Stock Return Forecasting." (2026).

Cao, X., Tao, J., Liu, Z., Lyu, R., & Li, J. (2026). Handling Missing Data in CALL: A Data Quality-Driven Imputation Framework for Learner Analytics. Future-Adaptive Intelligence and Lifelong Systems, 1 (1).

Abu Saleh, A., Siouris, S., Hughes, K., Yuan, R., & Pourkashanian, M. (2023). Assessment of mixtures of iso-pentanol and Jet A-1 for use in aviation gas turbine engines. In AIAA SCITECH 2023 Forum (p. 2341).